

Study of Flow Convergence in Rectangular Slots using Particle Shadowgraph Velocimetry

Yishak Yusuf¹, Shadi Ansari¹, Michael Bayans¹, Reza Sabbagh²,
Mouhammad El Hassan¹ and David S. Nobes^{1,*}

¹University of Alberta, Department of Mechanical Engineering, Edmonton, Canada

²RGL Reservoir Management Inc., Calgary, Canada

* david.nobes@ualberta.ca

Abstract

Motivated by the use of slotted liners in the production of bitumen steam assisted gravity drainage, this paper aims at quantifying the convergence phenomenon experienced by the flow as it enters these long aspect ratio apertures (slots) found on the lateral surface of these liners. A 2D measurement technique - particle shadowgraph velocimetry – was used to visualize the flow fields through rectangular channels manufactured to represent SAGD slots. The effects of the channel Reynolds number ($Re = 0.1$ to 10), and the width of the flow channel before the slot, on the curvature of the streamlines were studied. Results showed that the curvature in streamlines increased as the flow Reynolds number increased whereas an increase in wall distance led to lower curvature of streamlines.

1 Introduction

Steam-assisted gravity drainage (SAGD) is an enhanced oil recovery technique that produces oil by injecting steam into an oil sands formation that lowers the viscosity of bitumen to instigate its flow (Butler, 1994). The well completions, the piping system of the well, used in SAGD are manufactured to provide a pre-defined open area and flow conditions to prevent sand from being produced. This commonly involves including some form of perforation or screen that also minimizes sand production (Matanovic et al., 2012). Among the most common well completion methods used in SAGD are slotted liners (Leitch et al., 2018). Slotted liners are pipe casings that contain rectangular apertures (slots) on their lateral surface that are typically 0.3 to 0.5 mm wide (Xie et al., 2007) depending on the particle size distribution in the reservoir.

The performance of slotted liners can be drastically reduced due to plugging of the slots that results from one of a number of different failure mechanisms (Shen, 2013). The most common failure mechanisms are plugging by fines or sand particles, scale deposition, and fouling. The pressure distribution in the near-field flow domain has a direct effect on the transport phenomena involved and the reaction kinetics for precipitate formation (Vetter & Kandarpa, 1980).

On the production side of SAGD, the pressure drop in the flow can be primarily attributed to the contraction effects as the flow enters the narrow slots. The slots also induce a flow convergence phenomenon (Kaiser et al., 2002) which essentially represents the change in the shape (curvature) of the streamlines. Understanding this near-wellbore flow mechanics and the contributions of flow- and geometry-related design parameters is, therefore, of the utmost importance.

In a prior work by the authors, experiments were conducted to measure the pressure drop across rectangular orifices using test coupons (Yusuf et al., 2017). Results have shown that it is affected by the aspect ratio of the orifice. The model that was developed to characterize this pressure drop (Yusuf et al., 2017), can be described mathematically as:

$$\frac{\Delta P}{\frac{1}{2}\rho u^2} = [1 - \alpha^2] + (1 - \alpha) \left[\frac{2AR}{AR + 1} \right] \left[\frac{4\phi}{\sqrt{\pi} \cdot Re} \right] \quad (1)$$

where ΔP is the pressure drop across orifice, ρ is density of the fluid, u is the average streamwise velocity through the orifice, α is the ratio of the orifice cross sectional area to that of the pipe which it is installed in, AR is the aspect ratio of the rectangular orifice, Re is the Reynolds number of the flow, and ϕ is termed the flow convergence parameter. The Reynolds number was calculated using the average streamwise velocity and the hydraulic diameter of the rectangular orifice as the velocity and length scales, respectively.

Research activities are now focused on the convergence parameter, ϕ , with the ultimate goal of comprehensively describing its contribution to the pressure loss and determining its dependence on the geometry of the slot. As the development of Eq. 1 had the assumption of a 1D flow, complementing the findings with a technique that offers an additional plane of investigation was found to be necessary.

In this paper, the effect of channel geometry and Re on the flow convergence is investigated using 2D particle shadowgraph velocimetry (PSV). The main objective was to describe this phenomenon by using measurements that can visualize and quantify the flow convergence vis-à-vis the curvature of the streamlines. The setup used for the PSV experiments, the results obtained, and the main conclusions drawn are presented in the following sections of the paper.

2 Experiment

The setup used to conduct the PSV experiments and a flow cell used therein are shown in Figure 1. The setup, Figure 1 (a), mainly consisted of (1) flow channel assembly; (2) a syringe pump (PHD 2000, Harvard Apparatus); (3) a camera (SP-5000M-PMCL-CX; JAI Inc.) coupled with 50 mm lens (AF NIKKOR 50 mm 1:1.4D; Nikon); (4) an LED light source (BX0404-520 nm; Advanced Illumination); and (5) a function generator for controlling camera frame rate. The flow channel assembly, shown in Figure 1 (b), consisted of three laser-cut parts made from 6.35 mm thick acrylic sheets. The two outer parts were the windows that provided optical access for imaging whereas the middle part was the main flow cell containing the geometry being experimented. The wall distance, D , of the channel varied between 10 mm and 15 mm while the channel width, b , was kept constant at 3 mm. A syringe pump was used to drive the flow of glycerol which was seeded with 40 μm glass sphere particles (Dynoseeds ® TS 40, Microbeads). The camera which was run at 45 frames per second was used to capture images of the flow field that was illuminated by the LED source. The function generator had the sole purpose of achieving the required frame rate for the camera.

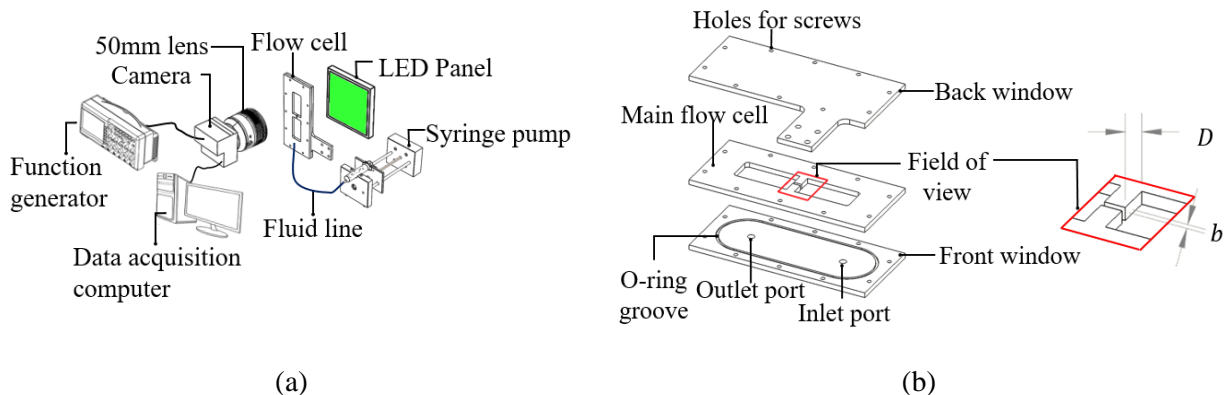


Figure 1 – (a) A representation of the experimental setup; and (b) the flow channel assembly consisting of laser-cut parts

Glycerol ($\mu = 1.4138 \text{ Pa}\cdot\text{s}$; $\rho = 1260.8 \text{ kg/m}^3$ at 20 °C) was selected as the working fluid to match the viscosity of bitumen at SAGD operating conditions. Four values of Re were covered in the experiments,

namely 0.1, 0.5, 5, and 10 by controlling the flow velocity. The velocity and length scales used to calculate Re were the average velocity through the channel and the width of the channel, respectively. As such, the range of Re covered matches with those pertaining to SAGD conditions which are in the range of 0.006 – 0.1 (Taubner et al., 2016).

A software built in-house on a commercial development environment (CVI LabWindows, National Instruments Inc.) ran on the data acquisition computer. The images acquired from experiments were then processed in commercial software (DaVis 8.4, LaVision GmbH) to determine the velocity field. A multi-pass scheme with specified interrogation window sizes was used in the processing of all experimental data. Windows of size 32×32 pixels for the first pass and 24×24 pixels for the second pass were used for the processing with 50% overlap. In the data processing stage that followed, the velocity field data was processed in a program built in a multi-paradigm computing environment (Matlab R2018a, Mathworks) to calculate the streamlines and other parameters within. This calculation determined the coordinates for each point along a streamline upon specification of a starting point.

3 Processing of experimental data

Samples of the raw images and the velocity field map that resulted from the processing are shown in Figure 2. The field of view for the experiments covered more of the region upstream the channel than downstream because the focus of the study was on investigating the convergence of the flow as it entered the channel. The seeding particles shown in the raw data, Figure 2 (a), were 2 – 3 pixels in size. Figure 2 (a) also shows that the coordinate system used in the analysis has its origin at entrance of the channel along the centerline.

The vector map in Figure 2(b) shows that the flow had the expected parabolic velocity distribution across the channel. The width of the channel, b , was used to normalize lengths along both directions in the plane. The distribution of the velocity, U , which was normalized by the global maximum velocity, U_{max} , showed that the maximum velocity in the channel occurs along the channel centerline.

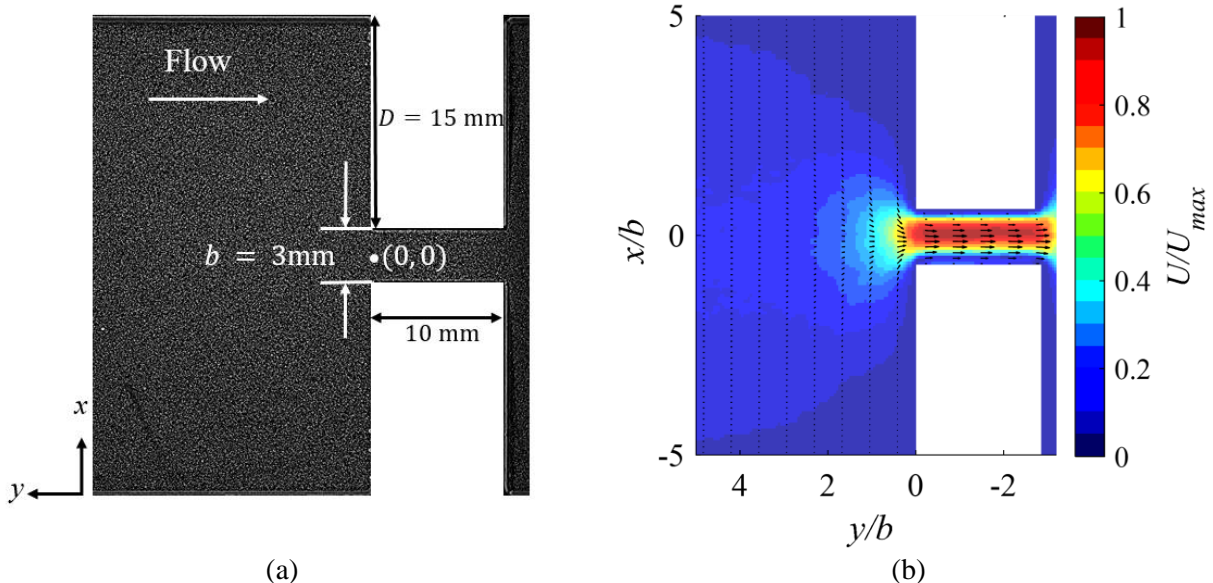


Figure 2 – (a) Raw image of the flow field; and (b) velocity vector from processing of data.

The velocity vector data that resulted from processing of images from PSV experiments were processed using custom written code to determine the streamlines for the flow field. Representative results from this stage of data processing are shown in Figure 3. The algorithm calculated the streamlines shown in Figure 3(a) when an initial position, x_0 , was specified. Figure 3(b) is included to demonstrate that the approach also allowed analysis on a single streamline in addition to groups of streamlines for the entire flow field. It

also offered control over a number of specifications such as length of a streamline, spacing between streamlines, the starting locations of the streamlines and the number of streamlines.

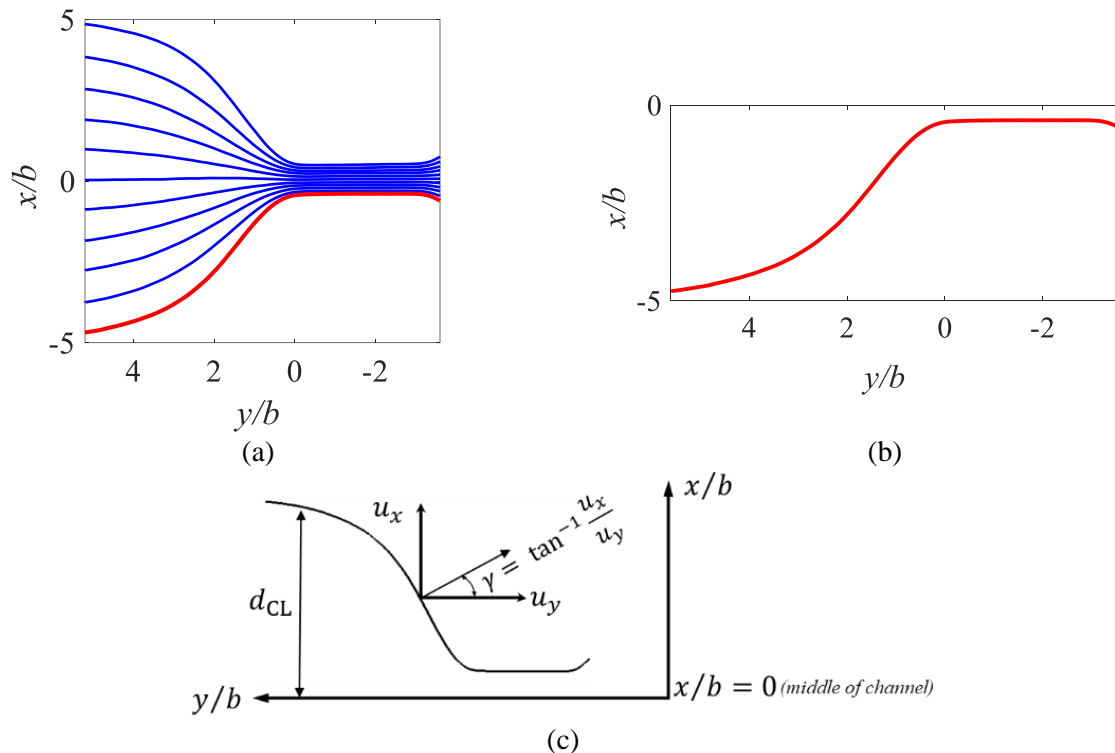


Figure 3 – (a) Streamlines in the whole flow field; (b) a single strand of a streamline; and (c) definition of centerline distance, d_{CL} , and angle between the normal and the horizontal

Two different parameters were used to quantify the curvature of the streamlines as shown in Figure 3 (c). The first parameter shown is d_{CL} which represented the distance between each streamline and the centerline of the channel. In the usage of this parameter it is assumed that the greater the distance, the more curvature, and hence increased flow convergence, required for a streamline to enter the channel. This will lead to the direct correlation between the distance d_{CL} and the flow convergence.

Also shown in Figure 3 (c) is γ which is defined as the angle between the normal to the streamline and the horizontal. Respective components of the velocity vectors at every point along a streamline were used to compute γ . This parameter could be used to determine streamline behaviors such as change in curvature and the location of inflection point of an individual streamline.

4 Results and discussion

Results from the analysis of experimental data are shown in Figure 4. The plots shown in Figure 4 (a) and (b) are for the flow through the channel where $D = 10$ mm whereas Figure 4 (c) and (d) are for the cases where $D = 15$ mm. Plots given in Figure 4 (a) and (c) can be used to compare the results for d_{CL} at different Re for the two wall distances. The results showed that Re had a visible effect on the flow convergence in the flow approaching the slot from the same location. In general, as Re increased, the streamlines shifted farther away from the centerline. This can entail streamlines for flows at relatively higher Re would require increased convergence to enter the channel than those at lower Re . Closer inspection also indicates that, for lower Re , the decrease in d_{CL} starts farther upstream than for higher Re . These observations were common to both values of the wall distance, D considered.

The progression of the flow convergence was also considered by looking at the change in γ along the flow as plotted in Figure 4 (b) and (d). The change in the angle had similar trends for all Re . The variation in the angle started at $\gamma \cong 0$ before the fluid approached the channel entrance where the streamlines were parallel to the centerline. The value of γ increased as the flow approached the channel entrance where the curvature in the streamlines started a continuous increase. After the flow had entered the channel, it was observed that γ begins to return towards zero as the streamlines became parallel to the centerline again.

The change in γ was also seen to be a function of the flow Re . As Re increased, γ reached its maximum at locations closer to the entrance of the slot for both wall distances. The location at which γ attained its maximum was also varied among the different wall distances, D , considered. It was seen that for the lower distance ($D = 10$ mm), shown in Figure 4 (b), the respective plots for γ reached maximum at locations where $y/b \cong 1$ whereas for larger wall distance (Figure 4d) the location was relatively farther from the inlet.

These results support the assumption that the difference in pressure drop for the flow through channels with constant cross sectional at different Re are due to the change in the curvature of the streamlines. It was also seen that lower wall distances led to higher curvature according to the maximum values of γ . Therefore, a greater pressure drop may be expected in cases with lower wall distance.

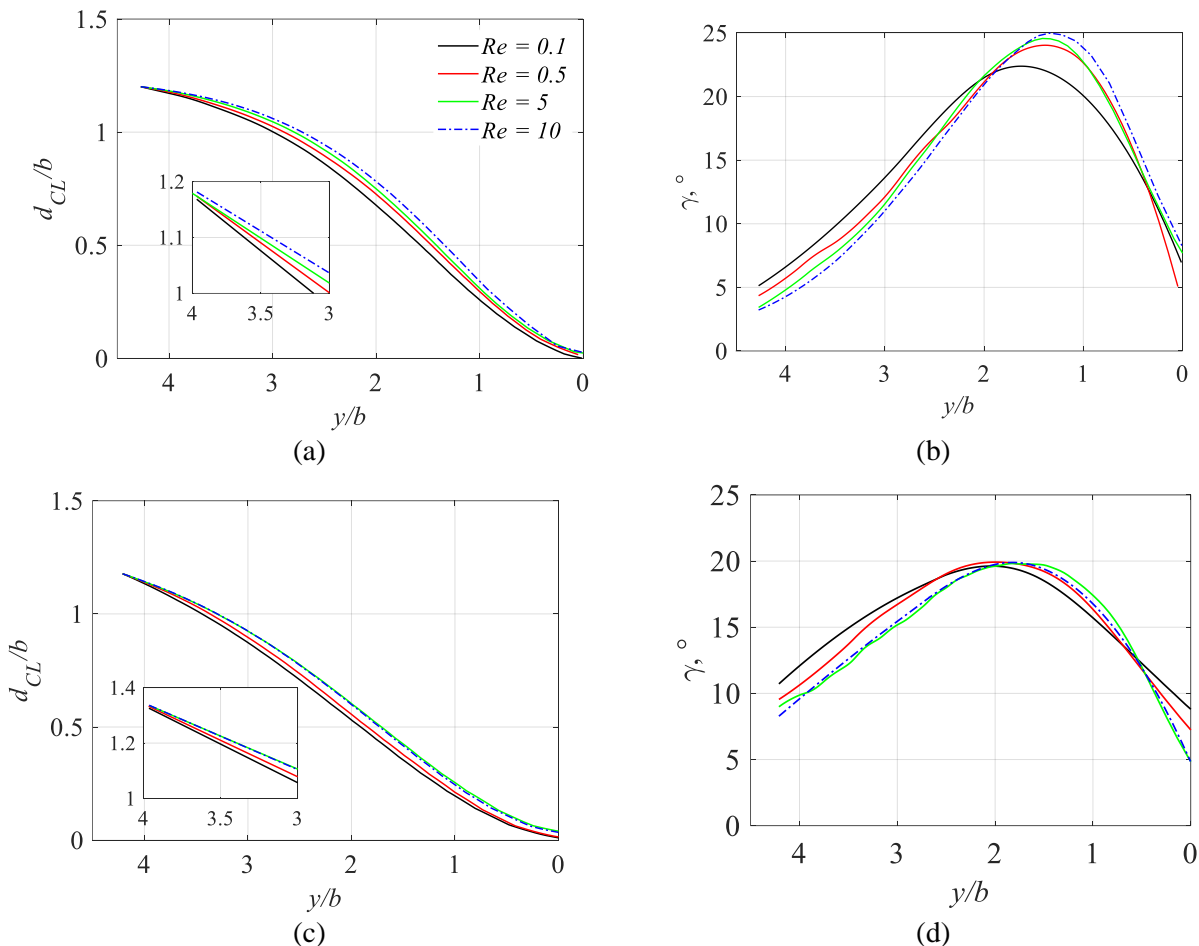


Figure 4 – Plots showing the variation in d_{CL} and γ for all distance $D = 10$ mm (a) – (b); and $D = 15$ mm (c) – (d) at the different Re

Conclusion

The flow convergence phenomenon in the flow through rectangular channels was investigated using a 2D measurement technique. Particle shadowgraph velocimetry was used to measure the velocity distribution in the flow field. Processed images from the experiment were used to calculate the streamlines. The variation in the parameters defined for the analysis in this study – d_{CL} and γ – were used to deduce about the effect of Re and wall distance on the curvature of the streamlines. In general, it was concluded that greater Re leads to greater curvature in the streamlines hence contributing to the pressure drop due to contraction. An inverse relationship was, however, observed between the wall distance and curvature of streamlines.

Acknowledgements

The authors gratefully acknowledge support from Natural Sciences and Engineering Research Council (NSERC) of Canada and RGL Reservoir Management Inc.

References

- Butler, R. M. (1994). Steam-assisted Gravity Drainage: Concept, Development, Performance, and Future. *Journal of Canadian Petroleum Technology*, 33(2), 44–50.
- Kaiser, T. M. V, Wilson, S., & Venning, L. A. (2002). Inflow Analysis and Optimization of Slotted Liners. *SPE Drilling and Completion*, 200–209.
- Leitch, M., Yusuf, Y., & Ma, Y. (2018). Interdisciplinary semantic model for managing the design of a steam-assisted gravity drainage tooling system. *Journal of Computational Design and Engineering*, 5(1), 68–79. <https://doi.org/10.1016/j.jcde.2017.11.004>
- Matanovic, D., Cikes, M., & Moslavac, B. (2012). *Sand control in well construction and operation*. Springer Science & Business Media.
- Shen, C. (2013). SAGD for Heavy Oil Recovery. In J. J. Sheng (Ed.), *Enhanced Oil Recovery Field Case Studies* (First Edit, pp. 413–445). Waltham: Gulf Professional Publishing. <https://doi.org/10.1016/B978-0-12-386545-8.00017-8>
- Taubner, S. P., Lipsett, M. G., Keller, A., & Kaiser, T. M. V. (2016). Gravity Inflow Performance Relationship for SAGD Production Wells. In *SPE Canada Heavy Oil Technical Conference* (pp. 1–18). Calgary.
- Vetter, O., & Kandarpa, V. (1980). Prediction of CaCO₃ scale under downhole conditions. In *SPE Fifth International Symposium on Oilfield and Geothermal Chemistry*. Stanford: Society of Petroleum Engineers. Retrieved from <https://www.onepetro.org/conference-paper/SPE-8991-MS>
- Xie, J., Jones, S. W., Matthews, C. M., Wagg, B. T., Parker, P., & Ducharme, R. (2007). Slotted liner design for SAGD wells. *World Oil*, 228(6), 67–75.
- Yusuf, Y., Baldygin, A., Sabbagh, R., Leitch, M., Waghmare, P. R., & Nobes, D. S. (2017). Effect of Aspect Ratio on Pressure Loss and Characteristics of Low Reynolds Number Flow Through Narrow Slots. In *Proceedings of the 2nd Thermal and Fluid Engineering Conference, TFEC2017 4th International Workshop on Heat Transfer, IWHT2017*. Las Vegas: American Society of Thermal and Fluid Engineers.
- Yusuf, Y., Sabbagh, R., & Nobes, D. S. (2017). Flow convergence model for flow through long aspect ratio rectangular orifices. In *Okanagan Fluid Dynamics Meeting* (pp. 145–152). August 21 -24 Kelowna, BC, Canada.